

Metal-Catalyst-Free Growth of Single-Walled Carbon Nanotubes on Substrates

Shaoming Huang,* Qiran Cai, Jiangying Chen, Yong Qian, and Lijie Zhang

Nanomaterials and Chemistry Key Laboratory, Wenzhou University, Wenzhou, 325027, P. R. China

Received December 9, 2008; E-mail: smhuang@wzu.edu.cn

It is well-known that metal nanoparticles (NPs) are indispensable for the growth of single-walled carbon nanotubes (SWNTs) by chemical vapor deposition (CVD). The Fe family of elements is known to be the most effective group of catalysts. However, in the past three years many other metal NPs such as Au,^{1–3} Ag,¹ Cu,^{1,4} Pd,¹ Rh,⁵ semiconductors NPs such as Si and Ge,³ carbides such as SiC³ and Fe₃C,⁶ and more recently Mg, Mn, Cr, Sn, and Al⁷ have been reported to be active for SWNT growth. These materials were hitherto regarded as inactive catalysts for the growth of CNTs in the past. Therefore, these findings challenge the traditional thinking about the growth of CNTs and the role of the catalysts. Furthermore, different types of catalysts will provide a greater understanding of the relationship between the catalysts and the structures of the SWNTs and thus may find out the approach for selective growth of semiconducting SWNTs (s-SWNTs) or metallic SWNTs (m-SWNTs). Pure s-SWNTs with uniform diameter and chirality are required for SWNT-based devices. A narrow (n, m) distribution of SWNTs grown from Fe–Ru and Co–Mo catalyst has been reported, indicating the dependence of the chirality of the SWNT on the type of catalyst.⁸ Here, we demonstrate almost any “small” particles regardless of their chemical composition can indeed catalyze the growth of SWNTs. Mechanically, rather than chemically, nanosized SiO₂ particles can be generated simply by scratching the surface of substrates (including quartz or Si wafer with SiO₂ layer) and prove for the first time that SiO₂ is an effective catalyst for the growth of SWNTs. Furthermore the SWNTs from SiO₂ NPs have a very narrow diameter distribution. More importantly, we have further proved that many other oxide NPs including Al₂O₃, TiO₂, and all lanthanide oxides except promethium oxide are also active for SWNT growth, indicating that the catalytic function of materials for SWNT growth is mainly size dependent. These new materials not only provide an alternative new type of catalysts for the growth of SWNTs, thus ruling out the relationship between the catalysts and SWNT structures, but also present candidates for investigating and understanding the role of the catalyst in the growth of SWNTs.

In a typical experiment, a clean Si wafer with a 1 μm layer of SiO₂ scratched by a diamond blade was used as substrate without putting any catalyst on the surface. CH₄-CVD or EtOH-CVD was carried out at 900 °C for 10 min [for detailed experiment, see Supporting Information (SI) S1]. To avoid possible metal contamination in the CVD system, a new quartz tube was used for every experiment. From SEM observations, nanotubes can be found around the edge of the scratched areas (several tens micrometers area) (Figure 1A–C). To further avoid possible catalytic effects from silicon,³ the same experiment was performed on a scratched quartz plate, and a similar result was obtained as shown in Figure 1D–F. The fact that no CNTs can be found on the nanoscopically smooth surfaces but the growth occurred on the scratched Si wafer/quartz plate under the same CVD conditions indicates the growth of SWNTs can only come from nanosized SiO₂ domains which are induced by scratching.

To verify the existence of nanosized SiO₂ particles, AFM was used to observe the area around the scratching line. It can be seen from Figure 2a that there are many particles with diameters less than 5 nm (there are many large particles as well). These SiO₂ NPs should come from the scratching because of the hardness of the substrate and are believed to be responsible for the growth of SWNTs. The AFM image and the size distribution of the CNTs according to the AFM height measurements are shown in Figure 2b and c. It can be seen that the SWNTs from SiO₂ have a very narrow

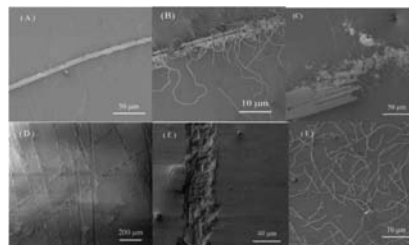


Figure 1. SEM images of SWNTs from the scratched substrates by diamond blade after CVD at 900 °C for 10 min: (A–C) Si wafer with 1 μm SiO₂ layer at different positions; (D–F) quartz plate with different magnifications.

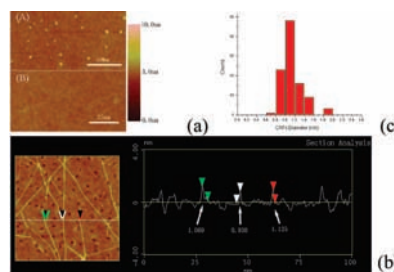


Figure 2. (a) AFM images of quartz plate after scratching (A) and bare quartz plate (B); (b) AFM image of SWNTs on scratched quartz plate and height measurement. (c) Size distribution of the SWNTs.

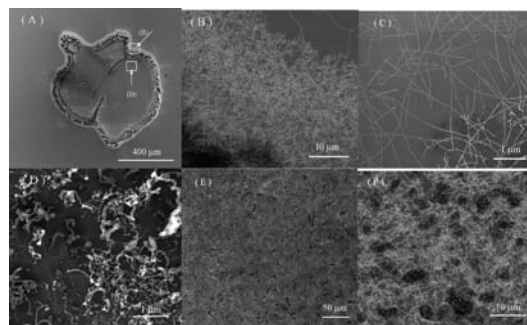


Figure 3. SEM images of the SWNTs on the Si wafer treated with HF followed by thermal annealing: (A) overview of the circle trace, (B) as indicated area B in A, (C) high magnification of B, (D) inner area of the circle, (E) quartz plate, (F) high magnification of E.

diameter distribution. A total of 100 SWNTs were measured, and 84% are in the range 0.8–1.4 nm. Near 50% are in the range 1.0–1.2 nm. Such a narrow distribution indicates that only SiO₂ with an appropriate size (<2 nm) is active for the growth of SWNTs.

To further avoid the effect of the diamond blade for the growth of SWNTs, we treated the substrates, both the Si wafer and quartz plate, with a HF aqueous solution followed by treatment in air at 1000 °C for 1 h [see SI]. On the silicon wafer, a circle trace was finally formed after drying as shown in Figure 3A because when the hydrophilic layer of SiO₂ was dissolved by HF, the aqueous solution shrank on the bottom silicon layer which is hydrophobic. Figure 3B is the area as indicated by the square in Figure 3A, and Figure 3C is the amplified image. From the SEM

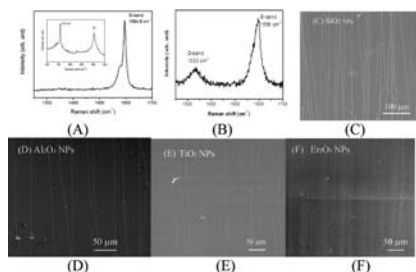


Figure 4. Raman spectra of (A) SWNTs within the circle trace area and (B) MWNTs or carbon filament inside the circle trace. SEM images of aligned long SWNT arrays from (C) SiO₂, (D) Al₂O₃, (E) TiO₂, and (F) Er₂O₃

images, highly dense random SWNTs can be clearly found around the whole circle trace. Inside the circle a number of carbon filaments or MWNTs can be found (Figure 3D). The effect of such treatment is that HF dissolves parts of the SiO₂ to break the SiO₂ layer on the top of the Si wafer and leave some small particles in the water drop. The formation of the circle trace with concentrated SiO₂ is due to the surface tension effect.⁹ On the quartz plate the whole substrate was covered by nanotubes as shown in Figure 3E and F because of the hydrophilic surface of the quartz plate. Raman spectra also indicate the difference between the circle trace and inner areas. Figure 4A is the Raman spectra of the SWNTs within the circle trace, showing a strong G-band peak at 1594 cm⁻¹ which is related to the Raman-allowed tangential G-mode of graphite and a radial breathing mode (RBM) at 157.5 cm⁻¹ (inserted image). Figure 4B is the Raman spectrum inside the circle, giving a broadened G-band and a wide D-band which contributes to the disordered carbon.

As reported recently, SiC NPs are an effective catalyst for SWNT growth.³ The current finding poses one question of the possibility of the formation of SiC NPs from the SiO₂ NPs under CVD conditions. Usually the formation of SiC from carbothermal reduction of SiO₂ requires a reductant and higher temperature (>1200 °C).¹⁰ Further XPS measurements on the wafer surface were performed. The binding energies of Si_{2p} on both the Si wafer (after HF treatment followed by thermal annealing at 1000 °C for 1 h) and quartz plate are ~102.8–103.5 eV which corresponds to SiO₂, and no silicon (98.8–99.5 eV) or silicon carbide (99.8–100.8 eV) was found on SWNT areas (the spot size of the X-ray is ~1 cm², and several spots were measured (see SI S3–S4)). For the Si wafer, it was thermally annealed and a layer of SiO₂ formed. The detectable depth of the X-ray on the Si surface is less than 5 nm. From the full spectrum of XPS there is no other metals such as Fe, Co, Ni that can be detected (SI S3). This result further confirms that SiO₂ acts as catalyst for the SWNT growth. Liu⁷ reported recently that SWNTs can be generated on ST-cut quartz by scratching a line on the substrate by steel and tungsten carbide blades; possibly not only the metal NPs from the blades but also SiO₂ NPs produced by scratching act as catalysts for SWNT growth.

Unlike metal catalysts such as the Fe-family of elements, SiO₂ does not have carbon solubility in the bulk phase and catalytic function to decompose hydrocarbon molecules. However, it is expected that the melting point (mp) of nanosized SiO₂ (<2 nm) will be lower than the growth temperature (mp of SiO₂: 1610 °C). We propose that nanosized SiO₂ is in a molten status at growth temperature and the high fluctuation of the liquid-like structure allows Si and O atoms to move around quickly, thus creating a space hole or dislocation. These space holes or dislocations might have the capability to catalytically decompose the hydrocarbon or ethanol molecules, and the high curvature of nanosized particles can be templates for the formation of a hemispherical cap with a graphitic structure for further SWNT growth. Because the mp of the NPs strongly depends on their size,¹³ we believe that the mp of SiO₂ is more size-dependent than metals such as Au and Ag. Only these smaller SiO₂ NPs (for example < 2 nm) are in the molten state and active for SWNT growth. This may be the reason why the SWNTs from SiO₂ NPs have a narrower diameter

distribution and may open a way to control the diameter of the SWNTs. According to this new understanding of the catalytic function of materials, we believe that the size of the catalysts (note: it is not limited to the traditional metal catalysts) is more important for SWNT growth. We speculate that any materials with a suitable size may be effective catalysts for SWNT growth. Nanosized SiO₂ prepared by a sol–gel method and some other oxides including Al₂O₃, TiO₂, and all lanthanide oxides except promethium oxide have been proven to be active for SWNT growth as well (will be published later). More oxides and other materials are being explored.

By applying fast-heating CVD¹¹ or using EtOH as a carbon source, long oriented SWNT arrays can be generated on a metal-catalyst-free quartz plate or Si wafer after scratching or using other oxide NPs including Al₂O₃, TiO₂, and lanthanide oxides (taking Er₂O₃ as an example) as catalysts (Figure 4C–F). As reported in our recent paper,¹² the structures of the long oriented SWNTs can be identified by using Raman spectroscopy and electrodeposition of the silver; thus the relationship between the oxide catalysts and the structures of long SWNTs from oxides is expected to be clarified. Further study is under investigation.

In summary, we have demonstrated that SiO₂ nanoparticles can be generated by simply scratching the quartz or silicon wafer with a SiO₂ layer and confirmed this to be active for the growth of SWNTs for the first time. Furthermore, the SWNTs from SiO₂ have a much narrower size distribution. This may open a way to control the diameter of the SWNTs. More importantly, our work has found a series of other oxides including Al₂O₃, TiO₂, and rare earth oxides to be active for SWNT growth as well. These new findings not only provide an alternative new type of catalysts for the growth of SWNTs but also give more insight into the role of the catalysts and a deeper understanding of the growth mechanism of SWNTs. The effective catalysts for SWNT growth seem to be more size-dependent than the catalysts. Long oriented SWNTs generated from these new catalysts enable us to rule out the relationship between the catalysts and the structures of the SWNTs. Thus controlled growth of SWNTs including the diameter and chirality is expected to be eventually realized.

Acknowledgment. The work was supported in part by grants from NSFC(50772076), MOST973 project(2007CB616901), ZJST(2006C24010), and WZST(H2005B022).

Supporting Information Available: Experimental details, SEM images of the SWNTs, and the XPS spectra. This material is available free of charge via the Internet at <http://pubs.acs.org>.

References

- (1) Takagi, D.; Homma, Y.; Hibino, H.; Suzuki, S.; Kobayashi, Y. *Nano Lett.* **2006**, *6* (12), 2642.
- (2) Bhavari, S.; Mile, E.; Steiner, S. A., III; Zare, A. T.; Dresselhaus, M. S.; Belcher, A. M.; Kong, J. *J. Am. Chem. Soc.* **2007**, *129*, 1516.
- (3) Takagi, D.; Kobayashi, Y.; Hibino, H.; Suzuki, S.; Homma, Y. *Nano Lett.* **2008**, *8* (3), 832.
- (4) Zhou, W.; Han, Z.; Wang, J.; Zhang, Y.; Jin, Z.; Sun, X.; Zhang, Y.; Yan, C.; Li, Y. *Nano Lett.* **2006**, *6* (12), 2987.
- (5) Ritschel, M.; Lenonhardt, A.; Elefant, D.; Oswald, S.; Büchner, B. *J. Phys. Chem. C* **2007**, *111*, 8414.
- (6) Yoshida, H.; Takeda, S.; Uchiyama, T.; Kohno, H.; Homma, Y. *Nano Lett.* **2008**, *8*, 2082.
- (7) Yuan, D.; Ding, L.; Chu, H.; Feng, Y.; McNicholas, T. P.; Liu, J. *Nano Lett.* **2008**, *8*, 2576.
- (8) (a) Li, Y.; Mann, D.; Rolandi, M.; Kim, W.; Ural, A.; Hung, S.; Javey, A.; Cao, J.; Wang, D.; Yenilmez, E.; Wang, Q.; Gibbons, J. F.; Nishi, Y.; Dai, H. *Nano Lett.* **2004**, *4*, 317. (b) Bachilo, S. M.; Balzano, L.; Herrera, J. E.; Pompeo, F.; Resasco, D. E.; Weisman, R. B. *J. Am. Chem. Soc.* **2003**, *125*, 11186.
- (9) Bunz, U. H. F. *Adv. Mater.* **2006**, *18*, 973.
- (10) Vix-Guterl, C.; Ehrburger, P. *Carbon* **1997**, *35*, 1587.
- (11) Huang, S.; Cai, X.; Liu, J. *J. Am. Chem. Soc.* **2003**, *125*, 5636. Huang, S.; Maynor, B.; Cai, X.; Liu, J. *Adv. Mater.* **2003**, *15*, 1651. Huang, S.; Woodson, M.; Smalley, R.; Liu, J. *Nano Lett.* **2004**, *4*, 1025.
- (12) Huang, S.; Qian, Y.; Cheng, J.; Cai, Q.; Wan, L.; Wang, S.; Hu, W. *J. Am. Chem. Soc.* **2008**, *130*, 11860.
- (13) Buffat, Ph.; Borel, J.-P. *Phys. Rev. A* **1976**, *13*, 2287.

JA809635S